ORGANOMETALLICS

pubs.acs.org/Organometallics

Article

Improving the Configurational Stability of Chiral-at-Iron Catalysts Containing Two *N*-(2-Pyridyl)-Substituted N-Heterocyclic Carbene Ligands

Nemrud Demirel, Jakob Haber, Sergei I. Ivlev, and Eric Meggers*

Cite This: *Organometallics* 2022, 41, 3852−3860

Read Online

ACCESS | Metrics & More | Article Recommendations | Supporting Information

ABSTRACT: Recently, we introduced the first example of chiral-at-iron catalysts in which two achiral *N*-(2-pyridyl)-substituted N-heterocyclic carbene (NHC) ligands in addition to two labile acetonitriles are coordinated around a central iron, to generate a stereogenic metal center [Hong, Y. et al. Chiral-at-Iron Catalyst: Expanding the Chemical Space for Asymmetric Earth-Abundant Metal Catalysis. *J. Am. Chem. Soc.* **2019**, *141*, 4569−4572]. A more facile synthesis of such chiral-at-iron catalysts was developed, which omits the use of expensive silver salts and an elaborate electrochemical setup. Configurational robustness was improved by replacing the imidazol-2-ylidene carbene moieties with benzimidazol-2-ylidenes. The π-acceptor properties of the altered NHCs were investigated by Ganter's ^{77}Se NMR method. The obtained benzimidazol-2-ylidene chiral-at-iron complex is an excellent catalyst for an asymmetric hetero-Diels−Alder reaction under open-flask conditions.

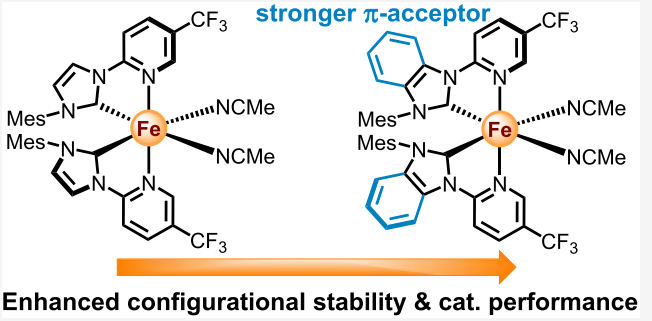

INTRODUCTION

With a rising interest in sustainable chemical synthesis,[1] the spotlight is on using earth-abundant rather than noble metals for the development of new transition-metal catalysts.[2] The earth-abundant metal iron is gaining particular attention due to its high abundance in the Earth's crust together with a low-toxicity profile.[3] Profound advancements have been achieved over the past two decades regarding asymmetric iron catalysis based on a comprehensive selection of chiral iron complexes.[4] Nevertheless, many challenges remain with respect to improving catalytic performance, identifying new iron catalyst scaffolds, discovering new catalytic processes, and establishing economic syntheses of such chiral iron catalysts.

The development of chiral transition-metal catalysts, including chiral iron catalysts, is predominately based on coordinating carefully tailored chiral ligands to a central metal. However, in a systematic research program, our group demonstrated the merit of chiral-at-metal catalysts in which the overall chirality is exclusively the consequence of a stereogenic metal center[5] with all coordinating ligands being achiral.[6−8] Our initial work was based on the noble metals iridium(III),[9] rhodium(III),[10] and ruthenium(II)[11] due to their intrinsically high configurational stability, which is at the heart of the chiral-at-metal design. Nonetheless, recently, we introduced the first examples of chiral iron catalysts consisting exclusively of achiral ligands and revealed their application to an asymmetric Cannizzaro reaction, a Nazarov cyclization, and hetero-Diels−Alder reactions.[12,13] In this catalyst scaffold, iron(II) is coordinated by two chelating *N*-(2-pyridyl)-substituted N-heterocyclic carbene ligands (PyNHC) in a C_2-symmetric manner, thereby providing a helical topology with a stereogenic iron center in the Λ (left-handed helicity) or Δ (right-handed helicity) configuration. Two acetonitriles complement the overall octahedral coordination sphere. In this design, the two PyNHC ligands are supposed to be configurationally inert to retain the stereochemical information, while the acetonitrile ligands are supposed to be labile to enable catalysis. This was facilitated by maximizing the ligand field stabilization energy by combining a strongly σ-donating NHC ligand with a π-accepting pyridine. At the same time, the acetonitrile ligands positioned *trans* to σ-donating NHC ligands are labilized due to the established *trans*-effect. Following this design, we achieved surprisingly robust configurational stabilities. Despite several modifications of the pyridyl substituents and changes in the mesityl group of the N-heterocyclic carbene, we observed that certain noncoordinating solvents, the presence of water, or the presence of air resulted in significant racemizations of the stereogenic iron center over time. We therefore became interested in under-

Received: September 29, 2022
Published: November 25, 2022

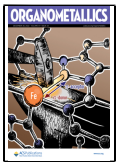

https://doi.org/10.1021/acs.organomet.2c00492
Organometallics 2022, 41, 3852−3860

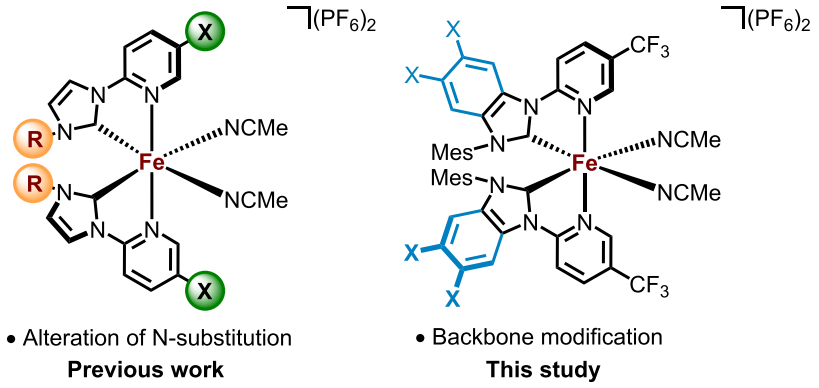

Figure 1. Previous work and this study regarding the design of chiral-at-metal catalysts.

Scheme 1. New Method for the Synthesis of Racemic Chiral-at-Iron Complexes

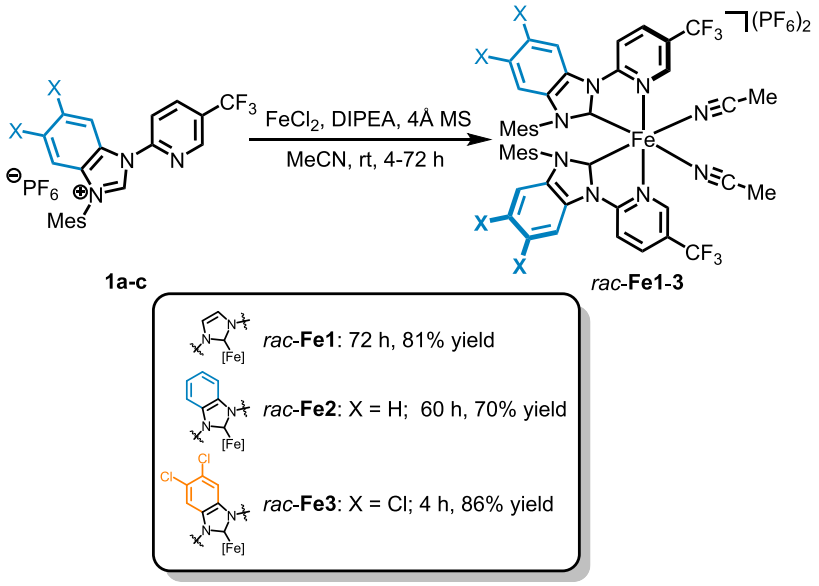

standing the parameters that determine the configurational stability of such chiral-at-iron complexes. Herein, we demonstrate the influence of the π-acceptor properties of the NHC ligands on the configurational stability. Replacing the imidazol-2-ylidene carbene moieties with benzimidazol-2-ylidenes provides a significantly more configurationally robust chiral-at-iron catalyst, which catalyzes an asymmetric hetero-Diels–Alder reaction with high stereoselectivity under open-flask conditions (Figure 1).

RESULTS AND DISCUSSION

Synthesis of Benzimidazol-2-ylidene Iron Complexes.

Previously, we accomplished the synthesis of the chiral-at-iron complexes under electrochemical conditions using a sacrificial iron anode in the presence of Ag_2O to generate silver carbene species and iron(II) in situ.[12,13] We aimed to develop a more convenient procedure without using expensive silver salts and a complicated electrochemical setup. Accordingly, the racemic complexes *rac*-**Fe1-3** were generated by deprotonation of the imidazolium salt **1a** or the benzimidazolium salts **1b,c** with Hünig's base (diisopropylethylamine, DIPEA) in MeCN using $FeCl_2$ as the iron source (Scheme 1). Using this protocol and a reaction time of 72 h, *rac*-**Fe1** was obtained in 81% yield compared to a yield of 70% following the previous electrochemical method.[12] The synthesis of the benzimidazol-2-ylidene complex *rac*-**Fe2** was achieved in 70% yield with a reaction time of 60 h, and the dichloro-substituted benzimidazol-2-ylidene complex *rac*-**Fe3** was provided in 86% yield after only a reaction time of 4 h. These results demonstrate that for achieving high yields, longer reaction times are required for less acidic imidazolium or benzimidazolium salts.

The racemic complexes *rac*-**Fe2** and *rac*-**Fe3** were resolved into their single enantiomers following our established chiral auxiliary method[14] (Scheme 2). Treatment of *rac*-**Fe2** or *rac*-**Fe3** with (*S*)-salicyloxazoline in the presence of Et_3N provided the complexes Λ-(*S*)-**Fe2** (41% yield) and Λ-(*S*)-**Fe3** (42% yield) as single diastereomers. Likewise, using (*R*)-salicyloxazoline instead provided the mirror-imaged complexes or Δ-(*R*)-**Fe2** (45% yield) and or Δ-(*R*)-**Fe3** (47% yield) after silica gel chromatography. Under the reaction conditions, (*S*)-salicyloxazoline does only form isolable complexes with Λ-**Fe2** or Λ-**Fe3**, while (*R*)-salicyloxazoline does only form isolable complexes with Δ-**Fe2** or Δ-**Fe3**. Indeed, unreacted enantioenriched complexes were isolated in the course of the silica gel chromatography but were not utilized further. Next, the diastereomerically pure iron auxiliary complexes were treated with NH_4PF_6 at 40 °C to replace the chiral bidentate ligands with acetonitriles to afford the individual enantiomers Λ-**Fe2** (86% yield), Δ-**Fe2** (91% yield), Λ-**Fe3** (80% yield),

https://doi.org/10.1021/acs.organomet.2c00492
Organometallics 2022, 41, 3852−3860

Scheme 2. Chiral Resolution of the Chiral-at-Iron Complexes

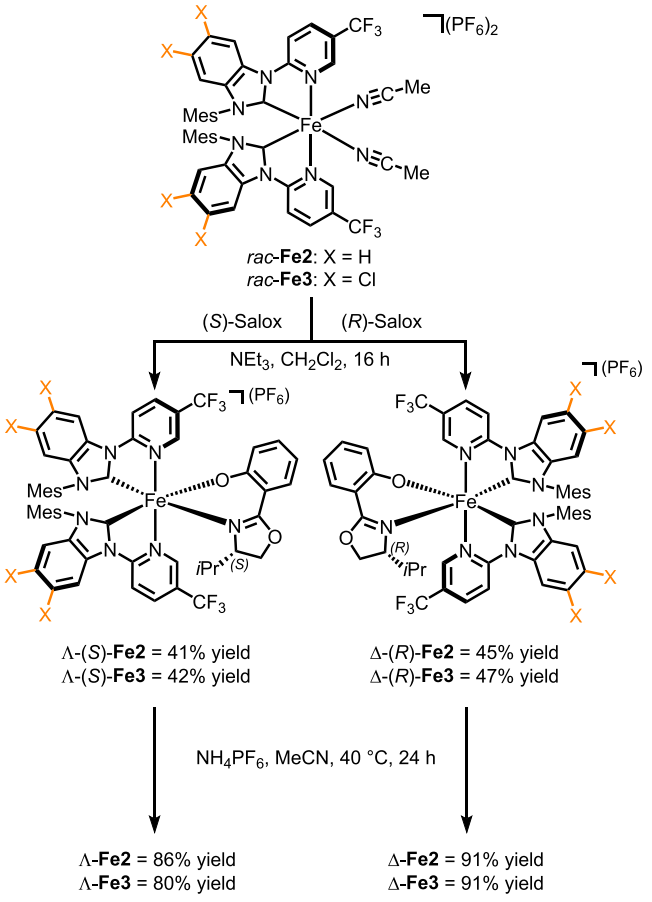

and Δ-**Fe3** (91% yield). The enantiopurity of these chiral-at-iron complexes was determined by converting them to their corresponding auxiliary complexes using the methyl instead of isopropyl substituted (*S*)- or (*R*)-salicyloxazoline. This allowed for both enantiomers to convert to stable diastereomeric metal complexes and diastereomeric excess and in turn enantiomeric excess was conveniently determined via ^{19}F NMR. As a result, for all of the nonracemic complexes, an ee of >99% was determined. CD spectra of the mirror-imaged complexes Λ- and Δ-**Fe2** are displayed in Figure 2.

Crystal Structure. Figure 3 displays a crystal structure of the racemic catalyst **Fe2**, which confirms the presence of a stereogenic iron center with a helical topology of the coordinated bidentate PyNHC ligands. The crystal structure also reveals a $\pi-\pi$ stacking of the mesityl substituents of the individual NHC ligands against the pyridyl moieties of the neighboring bidentate PyNHC ligands, which should contribute to the high constitutional and configurational stability of this class of chiral-at-iron complexes. The catalytic site is composed of the two labile acetonitrile ligands, while one methyl group of each mesityl moiety reaches toward the catalytic site and thus affects the asymmetric induction.

Catalysis of a Hetero-Diels–Alder Reaction. With enantiomerically pure chiral-at-iron complexes in hand, we tested the benzimidazol-2-ylidene complexes Λ-**Fe2** and Λ-**Fe3** in the previously reported hetero-Diels–Alder reaction of *β*,*γ*-unsaturated *α*-ketoester **3** with the dienophile 2,3-dihydrofuran **4** to afford the bicyclic dihydropyran **5** and compared with results obtained for the previously reported

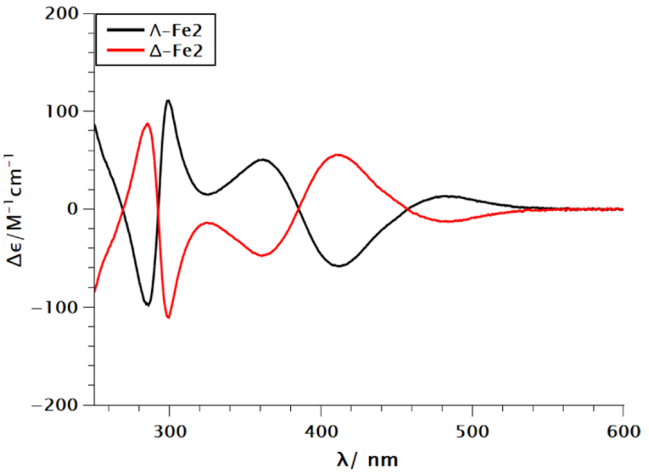

Figure 2. CD spectra of Λ-**Fe2** and Δ-**Fe2** recorded in MeCN (0.25 mM).

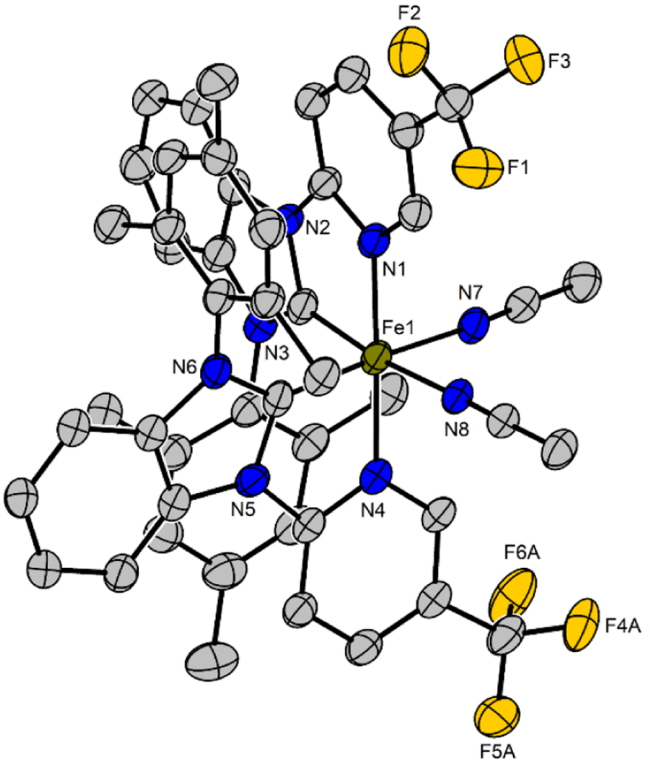

Figure 3. Crystal structure of *rac*-**Fe2** as an ORTEP drawing with 30% probability thermal ellipsoids at 100 K. The hexafluorophosphate counterions, hydrogens, and solvent molecules are omitted for clarity.

imidazol-2-ylidene catalyst Λ-**Fe1**.[13] To investigate the robustness of the catalysts, the reactions were performed either under air or under nitrogen and in the presence or absence of water (Table 1). As a result, all conducted reactions displayed high diastereoselectivity (>98:2) which will not be discussed further. Catalysis with Λ-**Fe1** under nitrogen atmosphere provided the dihydropyran **5** in 88% yield with 89.4% ee (entry 1). The presence of air did not affect the enantioselectivity but lowered somewhat the yield (71% yield, 89.6% ee) (entry 2), while the presence of small amounts of water (10 equivalents) diminished both yield and enantioselectivity (78% yield, 74.6% ee) (entry 3). Executing the reaction both in the presence of air and water afforded the hetero-Diels–Alder product also

https://doi.org/10.1021/acs.organomet.2c00492
Organometallics 2022, 41, 3852−3860

Table 1. Comparison of Different Chiral-at-Iron Catalysts in a Hetero-Diels–Alder Reaction[a]

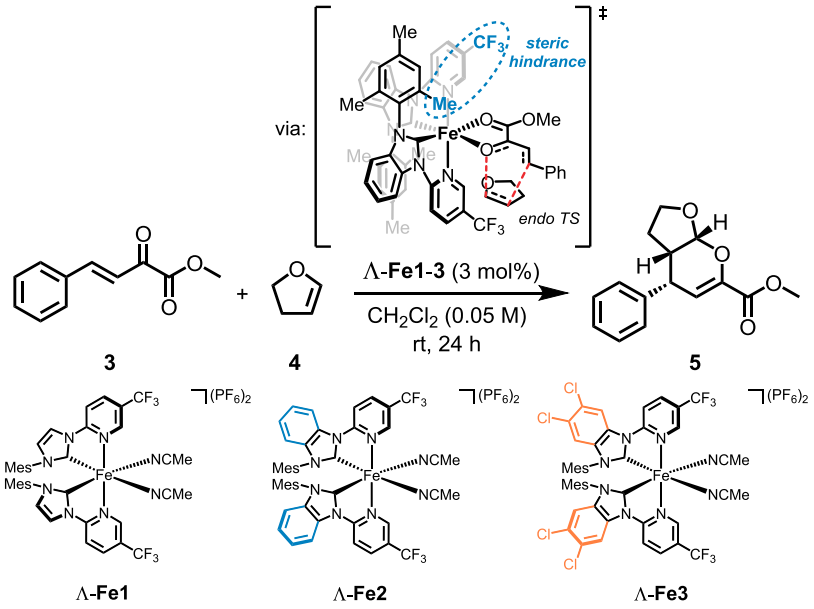

entry	catalyst	conditions	yield (%)[b]	dr[c]	ee (%)[c]
1	Λ-**Fe1**	N_2	88	97:3	89.4
2	Λ-**Fe1**	Air	71	97:3	89.6
3	Λ-**Fe1**	N_2 + H_2O (10 equiv)	78	97:3	74.6
4	Λ-**Fe1**	Air + H_2O (10 equiv)	67	98:2	81.2
5	Λ-**Fe2**	N_2	83	97:3	91.4
6	Λ-**Fe2**	Air	77	97:3	91.6
7	Λ-**Fe2**	N_2 + H_2O (10 equiv)	83	98:2	93.6
8	Λ-**Fe2**	Air + H_2O (10 equiv)	61	98:2	93.8
9	Λ-**Fe3**	N_2	64	95:5	70.8
10	Λ-**Fe3**	Air + H_2O (10 equiv)	38	99:1	89.0
11[d]	Λ-**Fe2**	Air + H_2O (10 equiv)	75	98:2	93.9
12	Δ-**Fe2**	Air + H_2O (20 equiv)	63	98:2	−94.1

[a]Reaction conditions: Λ-**Fe1**-**3** (3 mol %) or Δ-**Fe2** (3 mol %), ketoester **3** (0.20 mmol), and dihydrofuran **4** (0.30 mmol) were dissolved in distilled CH_2Cl_2 (0.05 M) and stirred under indicated conditions at room temperature for 24 h. [b]Isolated yield. [c]Values dr and ee were determined by HPLC analysis on a chiral stationary phase. [d]Catalyst at 5 mol % was used instead.

with a reduced yield and enantioselectivity (67% yield, 81.2% ee) (entry 4). From these experiments, we conclude that both water and air result in a slow decomposition and apparently water also leads to racemization of the iron catalyst Λ-**Fe1** during the catalysis. Surprisingly, when we conducted the same set of experiments with the catalyst Λ-**Fe2** (entries 5–8), the dihydropyran **5** was provided with high enantioselectivities under all conditions (91.4–93.8% ee) and the presence of water did not diminish the enantiomeric excess. In fact, water even slightly increased the ee value (91.4 vs 93.6% ee under nitrogen, 91.6 vs 93.8% ee under air). We also tested the dichlorinated benzimidazol-2-ylidene complex Λ-**Fe3** as a catalyst for the shown hetero-Diels–Alder reaction (entries 9 and 10), which showed a diminished performance compared to both Λ-**Fe1** and Λ-**Fe2**.

Overall, these results reveal that the benzimidazol-2-ylidene complex Λ-**Fe2** compared to the previously reported imidazol-2-ylidene complex Λ-**Fe1** is a significantly improved catalyst for the investigated hetero-Diels–Alder reaction. It provides higher enantioselectivity (proposed transition state in Table 1; see ref 13 for a discussion) and enables to perform the reaction under open-flask conditions since it is not sensitive to air or water. While we do not understand the slight increase in enantioselectivity in the presence of water, the modest decrease in yield in the presence of air can be attributed to a slow air-induced decomposition of the iron catalysts. However, increasing the catalyst loading of Λ-**Fe2** from 3 to 5 mol % could increase the yield of the dihydropyran product from 61 to 75% with no significant change in the stereoselectivity (entry 11). In addition, more water (20 instead of 10 equiv) using Δ-**Fe2** instead of Λ-**Fe2** (entry 12) gave a comparable reaction result to entry 8 (10 equivalents of water), providing the mirror-imaged product. Furthermore, the reduced catalytic performance of Λ-**Fe3** compared to Λ-**Fe2** in the hetero-Diels–Alder reaction indicates that additional electron-withdrawing groups on the benzimidazole, which further enhance the π-acceptor properties of the NHC, can ensure configurational robustness but also alter the catalytic behavior of the catalyst. Thus, if a certain degree of configurational stability is given, derivatization of the ligand could lead to a well-tailored catalyst for designated reactions.

Testing the Configurational Stability of the Chiral-at-Iron Catalysts. To experimentally verify the configurational stability of the chiral-at-iron complexes **Fe1**-**3**, enantiopure Δ-**Fe1**-**3** (all >99% ee) were stirred in CH_2Cl_2 + H_2O (1% v/v) under air for 24 h. Subsequently, they were reacted with

https://doi.org/10.1021/acs.organomet.2c00492
Organometallics 2022, 41, 3852–3860

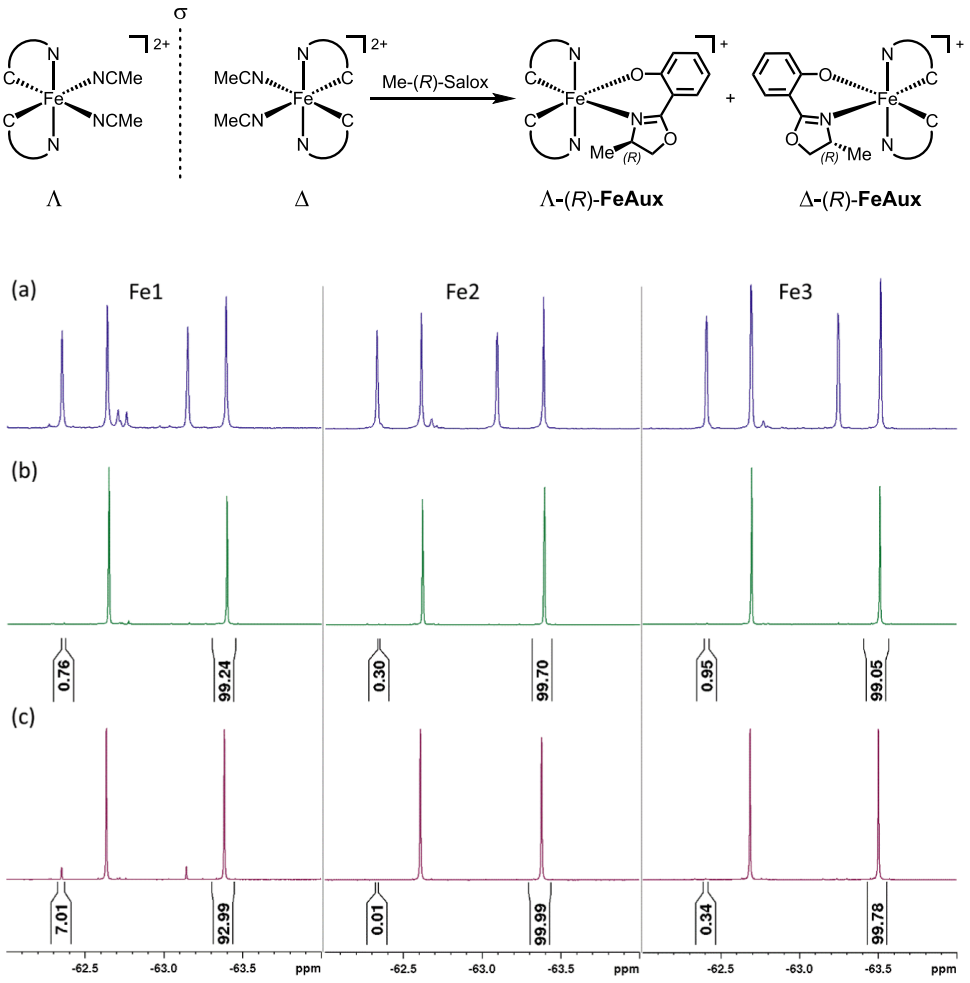

Figure 4. Evaluation of configurational stabilities. ^{19}F NMR spectra are shown after conversion to diastereomeric Λ-(*R*)- and Δ-(*R*)-**FeAux** complexes. (a) Auxiliary complexes obtained from racemic complexes **Fe1**-**3**. (b) Auxiliary complexes obtained from enantiopure complexes Δ-**Fe1**-**Fe3**. (c) Auxiliary complexes obtained from complexes Δ-**Fe1**-**Fe3** after stirring them in CH_2Cl_2 + H_2O (1% v/v) for 24 h. Further experimental details are provided in the Supporting Information.

Scheme 3. Characterization of the π-Acceptor Properties of Carbene Ligands via ^{77}Se NMR

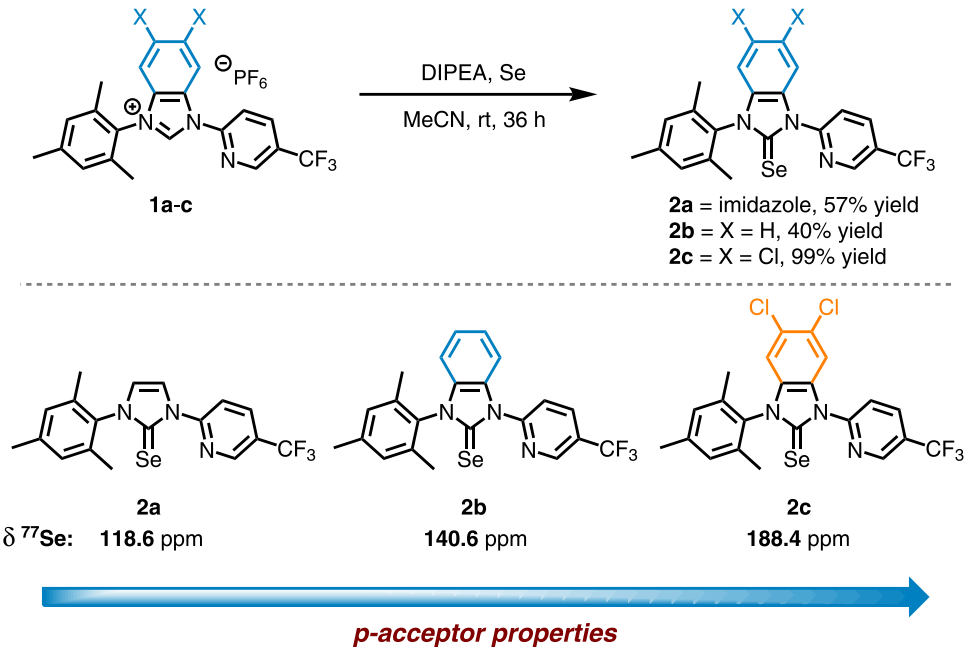

https://doi.org/10.1021/acs.organomet.2c00492
Organometallics 2022, 41, 3852−3860

methyl-substituted (*R*)-salicyloxazoline under basic conditions to obtain the corresponding auxiliary complexes **FeAux**, which are stable for both the Λ- and Δ-configured complexes and thus allow to determine the degree of racemization (Figure 4). This is demonstrated for a racemic (Figure 4a) and enantiomerically pure (Figure 4b) reference. In Figure 4c, the results of the racemization experiments are depicted, showing no racemization for Δ-**Fe2** (dr > 99:1 of the auxiliary complexes) and Δ-**Fe3** (dr > 99:1 of the auxiliary complexes) but a significant racemization for Δ-**Fe1** (dr 93:7 of the auxiliary complexes). By further prolonging the time to 48 h, only Δ-**Fe1** showed further racemization (dr 79:21 of the auxiliary complexes; see the Supporting Information for more information).

Investigation of π-Acceptor Properties of the NHC Ligands. To experimentally determine the electronic attributes, mainly the π-acceptor properties of the investigated ligands, Ganter's convenient ^{77}Se NMR method was chosen.[15] The imidazolium salts **1a**−**c** were converted to their selenium-NHC **2a**−**c** counterparts using a similar methodology as for the synthesis of the racemic iron(II) complexes (Scheme 3). Imidazolium salts **1a**−**c** were deprotonated using DIPEA and stirred with an excess of selenium in MeCN at room temperature for 36 h. Generation of the selenium-NHC via the use K_2CO_3 or NaHMDS failed.[16] The imidazolium-based PyNHC could be converted to the selenium analogue **2a** in 57% yield. Transformation of the benzimidazolium-derived PyNHCs was obtained in 40% yield (X = H, **2b**) and 99% yield for the dichloro-substituted congener (X = Cl, **2c**). With the selenium-NHC compounds **2a**−**c** in hand, ^{77}Se NMR measurements were conducted and the chemical shifts were compared. As a result, it becomes apparent that with an extended π-system of the benzimidazol-2-ylidene carbene (140.6 ppm, **2b**) and further addition of electron-withdrawing groups (188.4 ppm, **2c**), the π-acceptor properties increase gradually compared to the imidazol-2-ylidene carbene (118.6 ppm, **2a**).

CONCLUSIONS

In conclusion, we here reported an improved and very efficient access to a previously reported new class of chiral iron catalysts, so-called chiral-at-iron catalysts, omitting the use of expensive silver salts and an elaborate electrochemical setup. To achieve an improved configurational robustness, which is at the heart of the chiral-at-metal catalyst design, we investigated the π-acceptor properties of backbone-altered NHC ligands via their ^{77}Se NMR chemical shifts and their impact on the configurational stability of the stereogenic iron center. Configurational stability was improved significantly by replacing the imidazol-2-ylidene carbene moieties with benzimidazol-2-ylidenes. The obtained benzimidazol-2-ylidene chiral-at-iron complex **Fe2** was demonstrated to be an excellent catalyst for an asymmetric hetero-Diels−Alder reaction under open-flask conditions (presence of air and water). This design strategy paves the road for future structural motifs in the ligand sphere of chiral-at-iron catalysts providing distinct catalytic properties for applications in academia and industry, and still ensuring configurational robustness.

EXPERIMENTAL SECTION

General Methods and Materials. All reactions were carried out under a nitrogen atmosphere in oven-dried glassware unless noted otherwise. Solvents were distilled under nitrogen from calcium hydride (MeCN, CH_2Cl_2) prior to use. Reagents that were purchased from commercial suppliers were used without further purification. Flash column chromatography was performed with silica gel 60 M from Macherey−Nagel (irregular shaped, 230−400 mesh, pH 6.8, pore volume: 0.81 mL g^{-1}, mean pore size: 66 Å, specific surface: 492 m^2 g^{-1}, particle size distribution: 0.5% < 25 μm and 1.7% > 71 μm, water content: 1.6%). ^{1}H NMR, ^{13}C {^{1}H} NMR, ^{19}F{^{1}H} NMR, and ^{77}Se{^{1}H} NMR spectra were recorded on a Bruker AV NEO 300 MHz, AV II 300 MHz, AV III 500 MHz, or AV III HD 500 MHz spectrometer at ambient temperature. Chemical shift values δ are reported in ppm with the solvent resonance as internal standard. ^{19}F{^{1}H} NMR spectra were calibrated to trichlorofluoromethane ($CFCl_3$, δ = 0 ppm) as external standard. ^{77}Se{^{1}H} NMR spectra were calibrated to dimethyl selenide ($SeMe_2$, δ = 0 ppm) as external standard. IR spectra were recorded on a Bruker Alpha Fourier transform infrared (FT-IR) spectrometer. Chiral HPLC was performed on an Agilent 1200 or 1260. CD spectra were acquired with a JASCO J-810 CD spectropolarimeter (parameters: 600−200 nm, 1 nm bandwidth, 50 nm min^{-1} scanning speed, accumulation of 3 scans). High-resolution mass spectrometry was performed on a Finnigan LTQ-FT Ultra mass spectrometer (Thermo Fisher Scientific) using ESI or APCI as ionization source.

General Procedure for the Synthesis of Racemic Iron Complexes. Under nitrogen atmosphere, ligand **1a**−**c** (2.02 equiv), $FeCl_2$ (1.00 equiv), and 4 Å molecular sieves (1.0 g/mmol of **1a**−**c**) were dissolved in absolute and degassed acetonitrile (0.025 M based on **1a**−**c**) at rt and stirred for 5 min. Then, dry DIPEA (2.50 equiv) was added to the reaction mixture, which turned the colorless solution orange-red, and the mixture was stirred at room temperature for 4−72 h. The suspension was filtered over a short plug of celite, and the crude product was purified over silica gel column chromatography (CH_2Cl_2/MeCN 10:1 → 5:1) with a pad of NH_4PF_6 on top, to ensure complete elution of the desired product. To completely remove the remaining NH_4PF_6 and DIPEA·HPF_6 salt, the complex was dissolved in CH_2Cl_2/MeCN (10:1) and washed with H_2O (3×), dried over Na_2SO_4, and filtered over a short plug of celite. The solvent was removed under reduced pressure to afford the desired products *rac*-**Fe1**-**Fe3**. The iron complex *rac*-**Fe1** has been reported previously, and the analytical data are in agreement with the literature.[12]

rac-Fe1. Following the general procedure, *rac*-**Fe1** (185 mg, 0.17 mmol, 81%) was obtained as a red solid from the corresponding ligand **1a** (0.20 g, 0.42 mmol). *rac*-**Fe1** still contains some DIPEA·HPF_6-salt, since aq. work-up leads to some degradation of the complex. ^{1}H NMR (300 MHz, CD_3CN): δ = 8.37 (s, 2H), 8.29 (s, 2H), 8.07 (d, *J* = 8.6 Hz, 2H), 7.65 (d, *J* = 8.7 Hz, 2H), 7.21 (s, 2H), 6.71 (s, 2H), 6.62 (s, 2H), 2.16 (s, 3H), 1.99 (s, 3H), 1.46 (s, 3H) ppm. ^{19}F NMR (282 MHz, CD_3CN): δ = −62.86 (s, CF_3), −72.89 (d, $J_{P,F}$ = 706.4 Hz, PF_6) ppm. ^{13}C NMR (125 MHz, CD_3CN): δ = 200.15, 158.11, 150.99 ($J_{C,F}$ = 4.5 Hz), 140.86, 137.53 ($J_{C,F}$ = 3.2 Hz), 135.95, 134.69, 134.24, 132.60, 130.46, 130.39, 129.81, 124.94 ($J_{C,F}$ = 34.9 Hz), 123.44 ($J_{C,F}$ = 271.8 Hz), 120.43, 112.37, 20.81, 17.52, 17.40 ppm.

rac-Fe2. Following the general procedure, *rac*-**Fe2** (158 mg, 0.13 mmol, 70%) was obtained as an orange solid from the corresponding ligand **1b** (0.20 g, 0.38 mmol). ^{1}H NMR (300 MHz, CD_3CN): δ = 8.50 (s, 2H), 8.24 (t, *J* = 8.6 Hz, 2H), 8.10 (d, *J* = 8.9 Hz, 2H), 7.64 (t, *J* = 8.0 Hz, 2H), 7.43 (t, *J* = 7.7 Hz, 2H), 6.80 (s, 2H), 6.75 (d, *J* = 8.0 Hz, 2H), 6.71 (s, 2H), 2.24 (s, 3H), 1.96 (s, 3H, underneath the CD_3CN-signal), 1.00 (s, 3H) ppm. ^{13}C NMR (125 MHz, CD_3CN): δ = 214.20, 158.66, 150.87 ($J_{C,F}$ = 4.5 Hz), 141.75, 138.88, 137.90 ($J_{C,F}$ = 3.2 Hz), 136.65, 135.18, 132.76, 132.59, 131.14, 130.95, 130.77, 127.06, 126.55, 124.73 ($J_{C,F}$ = 34.7 Hz), 123.42 ($J_{C,F}$ = 271.2 Hz), 113.41, 113.13, 111.74, 20.94, 17.48, 17.00 ppm. ^{19}F NMR (282 MHz, CD_3CN): δ = −62.77 (s, CF_3), −72.94 (d, $J_{P,F}$ = 706.3 Hz, PF_6) ppm. IR (neat): $\tilde{\nu}$ = 2925 (w), 2297 (w), 1623 (w), 1605 (w), 1503 (w), 1473 (w), 1403 (m), 1324 (s), 1269 (w), 1218 (w), 1173 (w), 1137 (m), 1111 (w), 1085 (m), 1040 (w), 929 (w), 830 (s), 746 (m), 671 (w), 644 (w), 612 (w), 557 (s), 462 (w), 432 (w) cm^{-1}. HRMS ESI; *m*/*z* calcd for $C_{48}H_{42}F_6Fe_1N_8$ $[M]^{2+}$: 450.1388, found: 450.1390.

https://doi.org/10.1021/acs.organomet.2c00492
Organometallics 2022, 41, 3852−3860

*rac-**Fe3***. Following the general procedure, *rac*-**Fe3** (479 mg, 0.36 mmol, 86%) was obtained as an orange solid from the corresponding ligand **1c** (0.50 g, 0.84 mmol). ^{1}H NMR (300 MHz, CD_3CN): δ = 8.49 (s, 2H), 8.44 (s, 2H), 8.23 (d, J = 7.7 Hz, 2H), 8.08 (d, J = 8.8 Hz, 2H), 6.96 (s, 2H), 6.80 (s, 2H), 6.73 (s, 2H), 2.24 (s, 3H), 1.95 (s, 3H, underneath the CD_3CN-signal), 1.10 (s, 3H) ppm. ^{13}C NMR (125 MHz, CD_3CN): δ = 216.99, 157.74, 150.94 ($J_{C,F}$ = 4.5 Hz), 142.14, 138.26, 138.24, 136.64, 135.16, 133.12, 131.56, 131.53, 131.32, 131.01, 130.88, 130.25, 125.24 ($J_{C,F}$ = 34.7 Hz), 123.26 ($J_{C,F}$ = 272.0 Hz), 114.61, 113.81, 113.12, 20.96, 17.48, 17.26 ppm. ^{19}F NMR (282 MHz, CD_3CN): δ = −62.81 (s, CF_3), −72.95 (d, $J_{P,F}$ = 706.3 Hz, PF_6) ppm. IR (neat): $\tilde{\nu}$ = 2924 (w), 1624 (w), 1503 (w), 1467 (w), 1425 (w), 1400 (w), 1327 (s), 1303 (w), 1279 (w), 1200 (w), 1171 (w), 1140 (m), 1111 (w), 1085 (m), 1039 (w), 1006 (w), 986 (w), 948 (w), 926 (w), 832 (s), 753 (w), 703 (w), 685 (w), 664 (w), 624 (w), 600 (w), 558 (m), 511 (w), 490 (w), 453 (w) cm^{-1}. HRMS ESI; m/z calcd for $C_{48}H_{38}Cl_4F_6Fe_1N_8$ $[M]^{2+}$: 519.0599, found: 519.0583.

General Procedure for the Synthesis of Auxiliary Complexes. Under nitrogen, a flame-dried Schlenk tube was charged with *rac*-**Fe2-3** (1.00 equiv) and (*S*)- or (*R*)-Salox (1.00 equiv). The solids were dissolved in dry CH_2Cl_2 (0.05 M) and NEt_3 (1.50 equiv) was added. The reaction was stirred at 40 °C for 16 h. Afterward, the mixture was concentrated under reduced pressure and the residue was purified by silica gel column chromatography (CH_2Cl_2/MeCN 50:1 → 25:1) to afford the desired auxiliary complex Λ-(*S*)- or Δ-(*R*)-**Fe2-3**. The unreacted enantioenriched Δ- or Λ-**Fe2-3** was then eluted (CH_2Cl_2/MeCN 10:1 → 5:1) and can be further purified by converting it with (*R*)- or (*S*)-Salox.

*Δ-(R)-**Fe2** and Λ-(S)-**Fe2***. Following the general procedure, Δ-(*R*)-**Fe2** (53.0 mg, 0.045 mmol, 45%) was obtained as a dark orange solid from the corresponding *rac*-**Fe2** (120 mg, 0.101 mmol). Λ-(*S*)-**Fe2** (39.5 mg, 0.034 mmol, 41%) was obtained in an analogous fashion as a dark orange solid from *rac*-**Fe2** (97.5 mg, 0.082 mmol). Analytical data for Δ-(*R*)-**Fe2**: ^{1}H NMR (300 MHz, CD_2Cl_2): δ = 8.85 (s, 1H), 8.15 (d, J = 8.3 Hz, 1H), 8.08 (d, J = 8.2 Hz, 1H), 8.00−7.88 (m, 4H), 7.79 (d, J = 8.7 Hz, 1H), 7.57 (q, J = 8.8 Hz, 2H), 7.39−7.33 (m, 3H), 6.90 (t, J = 7.8 Hz, 1H), 6.82 (s, 1H), 6.71 (s, 2H), 6.64 (t, J = 7.2 Hz, 2H), 6.48 (s, 1H), 6.42 (d, J = 8.6 Hz, 1H), 6.24 (t, J = 7.4 Hz, 1H), 4.42−4.39 (m, 1H), 4.24 (t, J = 8.9 Hz, 1H), 3.82−3.79 (m, 1H), 2.28 (s, 3H), 2.17 (s, 3H), 2.12 (s, 3H), 2.06 (s, 3H), 1.11 (s, 3H), 0.92 (s, 3H), 0.43 (d, J = 6.9 Hz, 3H), 0.11 (d, J = 6.7 Hz, 3H), −0.32 (quint, J = 7.3 Hz, 1H) ppm. ^{13}C NMR (125 MHz, CD_2Cl_2): δ = 221.78, 219.43, 172.99, 167.75, 159.21, 158.77, 150.63 ($J_{C,F}$ = 4.8 Hz), 150.44 ($J_{C,F}$ = 4.5 Hz), 140.88, 140.84, 139.27, 138.44, 137.49, 135.10, 134.97, 134.88 ($J_{C,F}$ = 3.2 Hz), 134.77 ($J_{C,F}$ = 3.2 Hz), 134.45, 134.41, 131.85, 131.72, 131.07, 131.04, 130.89, 130.52, 130.25, 129.93, 129.43, 126.02, 125.45, 125.19, 123.91, 123.14 ($J_{C,F}$ = 34.3 Hz), 122.92 ($J_{C,F}$ = 272.1 Hz), 122.65 ($J_{C,F}$ = 272.1 Hz), 122.06 ($J_{C,F}$ = 34.3 Hz), 113.63, 111.70, 111.35, 111.11, 110.55, 110.54, 110.00, 74.55, 71.91, 70.34, 67.33, 30.39, 20.87, 20.69, 18.93, 18.15, 17.54, 17.14, 16.80, 13.92 ppm. ^{19}F NMR (282 MHz, CD_2Cl_2): δ = −62.78 (s, CF_3), −63.40 (s, CF_3), −73.13 (d, $J_{P,F}$ = 710.5 Hz, PF_6) ppm. IR (neat): $\tilde{\nu}$ = 2966 (w), 2926 (w), 1611 (m), 1583 (w), 1539 (w), 1500 (w), 1471 (m), 1446 (w), 1398 (m), 1328 (s), 1313 (w), 1257 (m), 1231 (w), 1212 (w), 1169 (w), 1137 (m), 1108 (w), 1083 (m), 1033 (w), 993 (w), 960 (w), 928 (w), 839 (s), 746 (m), 694 (w), 667 (w), 611 (w), 558 (m), 462 (w), 432 (w) cm^{-1}. HRMS APCI; m/z calcd for $C_{56}H_{50}F_6Fe_1N_7O_2$ $[M]^{+}$: 1022.3276, found: 1022.3283.

*Δ-(R)-**Fe3** and Λ-(S)-**Fe3***. Following the general procedure, Δ-(*R*)-**Fe3** (37.5 mg, 0.029 mmol, 47%) was obtained as a dark orange solid from *rac*-**Fe3** (81.0 mg, 0.061 mmol). Λ-(*S*)-**Fe3** (82.5 mg, 0.063 mmol, 42%) was obtained in an analogous fashion as a dark orange solid from *rac*-**Fe3** (200 mg, 0.151 mmol). Analytical data for Δ-(*R*)-**Fe3**: ^{1}H NMR (300 MHz, CD_2Cl_2): δ = 8.82 (s, 1H), 8.29 (s, 1H), 8.22 (s, 1H), 8.03 (d, J = 8.6 Hz, 1H), 7.88 (d, J = 9.0 Hz, 1H), 7.85-7.78 (m, 3H), 7.34 (d, J = 7.9 Hz, 1H), 6.91 (t, J = 7.7 Hz, 1H), 6.85 (s, 1H), 6.78-7.76 (m, 4H), 6.53 (s, 1H), 6.42 (d, J = 8.5 Hz, 1H), 6.27 (t, J = 7.4 Hz, 1H), 4.43 (d, J = 9.1 Hz, 1H), 4.25 (t, J = 9.1 Hz, 1H), 3.78 (d, J = 7.7 Hz, 1H), 2.29 (s, 3H), 2.17 (s, 3H), 2.16 (s, 3H), 2.08 (s, 3H), 1.22 (s, 3H), 1.03 (s, 3H), 0.45 (d, J = 6.9 Hz, 3H), 0.10 (d, J = 6.6 Hz, 3H), −0.43 (quint, J = 7.2 Hz, 1H) ppm. ^{13}C NMR (125 MHz, CD_2Cl_2): δ = 224.35, 221.83, 172.73, 167.95, 158.14, 157.65, 150.62 ($J_{C,F}$ = 5.3 Hz), 150.44 ($J_{C,F}$ = 4.6 Hz), 141.66, 141.61, 138.56, 137.73, 137.22, 135.80 ($J_{C,F}$ = 3.2 Hz), 135.56 ($J_{C,F}$ = 3.5 Hz), 134.79, 134.72, 134.70, 133.98, 131.34, 131.13, 130.91, 130.72, 130.62, 130.41, 130.37, 130.31, 130.22, 129.99, 129.47, 128.81, 128.80 ($J_{C,F}$ = 34.4 Hz), 122.74 ($J_{C,F}$ = 34.5 Hz), 122.67 ($J_{C,F}$ = 272.7 Hz), 122.39 ($J_{C,F}$ = 272.6 Hz), 114.14, 113.27, 111.67, 111.47, 110.98, 110.94, 110.84, 74.52, 67.49, 30.49, 20.87, 20.69, 18.97, 18.14, 17.57, 17.33, 16.89, 13.89 ppm. ^{19}F NMR (282 MHz, CD_2Cl_2): δ = −62.87 (s, CF_3), −63.53 (s, CF_3), −72.81 (d, $J_{P,F}$ = 710.8 Hz, PF_6) ppm. IR (neat): $\tilde{\nu}$ = 2965 (w), 2926 (w), 1610 (m), 1583 (w), 1540 (w), 1498 (w), 1485 (w), 1466 (m), 1445 (w), 1417 (w), 1394 (m), 1326 (s), 1303 (w), 1256 (m), 1231 (w), 1213 (w), 1166 (w), 1139 (m), 1110 (w), 1082 (m), 1031 (w), 1002 (w), 986 (w), 955 (w), 928 (w), 918 (w), 837 (s), 753 (w), 710 (w), 702 (w), 685 (w), 664 (w), 626 (w), 599 (w), 574 (w), 557 (m), 534 (w), 509 (w), 489 (w), 453 (w), 427 (w) cm^{-1}. HRMS APCI; m/z calcd for $C_{56}H_{46}Cl_4F_6Fe_1N_7O_2$ $[M]^{+}$: 1160.1700, found: 1160.1701.

General Procedure for the Auxiliary Cleavage. A Schlenk flask was charged with Λ-(*S*)- or Δ-(*R*)-**Fe2-3** (1.00 equiv) and NH_4PF_6 (10 equiv) set under nitrogen. Then, the solids were dissolved in MeCN (3.60 mL) and stirred for 24 h at 40 °C. Afterward, the solvent was removed under reduced pressure and the residue was transferred to a silica gel column (CH_2Cl_2/MeCN 10:1 → 5:1) to afford the corresponding Λ- or Δ-iron complexes.

*Λ-**Fe2***. According to the general procedure, Λ-**Fe2** (34.5 mg, 0.029 mmol, 86%) was obtained as an orange solid from the corresponding Λ-(*S*)-**Fe2** (39.5 mg, 0.034 mmol). CD (CH_3CN): λ, nm ($\Delta\varepsilon$, $M^{-1}cm^{-1}$) 285 (−97), 299 (+110), 325 (+16), 361 (+50), 412 (−58), 482 (+13).

*Δ-**Fe2***. According to the general procedure, Δ-**Fe2** (48.6 mg, 0.041 mmol, 91%) was obtained from the corresponding Δ-(*R*)-**Fe2** (52.3 mg, 0.045 mmol). CD (CH_3CN): λ, nm ($\Delta\varepsilon$, $M^{-1}cm^{-1}$) 285 (+87), 299 (−110), 325 (−14), 361 (−47), 412 (+56), 482 (−13).

*Λ-**Fe3***. Following the general procedure, Λ-**Fe3** (67.4 mg, 0.051 mmol, 80%) was obtained as an orange solid from the corresponding Λ-(*S*)-**Fe3** (82.5 mg, 0.063 mmol). CD (CH_3CN): λ, nm ($\Delta\varepsilon$, $M^{-1}cm^{-1}$) 287 (−94), 300 (+64), 322 (+24), 360 (+78), 409 (−74), 482 (+17).

*Δ-**Fe3***. According to the general procedure, Δ-**Fe3** (40.0 mg, 0.030 mmol, 91%) was obtained from the corresponding Δ-(*R*)-**Fe3** (43.1 mg, 0.033 mmol). CD (CH_3CN): λ, nm ($\Delta\varepsilon$, $M^{-1}cm^{-1}$) 287 (+109), 300 (−75), 322 (−28), 360 (−90), 409 (+85), 482 (−19).

General Procedure for the Synthesis of Selenium-NHC Products. A Schlenk tube was charged with compounds **1a−c** (1.00 equiv), gray selenium (3.00 equiv), and 4 Å molecular sieves (1.0 g/mmol of **1a−c**), and then the flask was purged with nitrogen. Then, distilled and degassed MeCN (0.05 M) was added at rt and stirred for 5 min. Then, dry DIPEA (3.00 equiv) was added to the reaction mixture and stirred at room temperature for 36 h. Afterward, the reaction mixture was filtered over a short plug of silica with CH_2Cl_2 to afford the desired selenium products **2a−c**.

*1-Mesityl-3-(5-(trifluoromethyl)pyridin-2-yl)-1,3-dihydro-2H-imidazole-2-selenone (**2a**).* Following the general procedure, selenium-imidazole **2a** (24.5 mg, 0.06 mmol, 57%) was obtained as an off-white solid from the corresponding imidazolium **1a** (50.0 mg, 0.10 mmol). ^{1}H NMR (300 MHz, $CDCl_3$): δ = 9.71 (d, J = 8.7 Hz, 1H), 8.80 (s, 1H), 8.12 (d, J = 8.6 Hz, 1H), 8.02 (s, 1H), 7.03 (s, 2H), 6.93 (s, 1 H), 2.36 (s, 3H), 2.10 (s, 6H) ppm. ^{13}C NMR (75 MHz, $CDCl_3$): δ = 157.69, 152.95, 145.58 ($J_{C,F}$ = 4.1 Hz), 139.82, 135.54, 135.33 ($J_{C,F}$ = 3.3 Hz), 134.11, 129.53 (2C), 125.74 ($J_{C,F}$ = 33.5 Hz), 123.34 ($J_{C,F}$ = 272.3 Hz), 120.50, 119.13, 118.15, 21.34, 18.28 (2C) ppm. ^{19}F NMR (282 MHz, $CDCl_3$): δ = −62.20 (s, CF_3) ppm. ^{77}Se NMR (57 MHz, $CDCl_3$): δ = 118.60 (s, C═*Se*) ppm. IR (neat): $\tilde{\nu}$ = 3159 (w), 3122 (w), 3089 (w), 2920 (w), 2853 (w), 1606 (m), 1581 (w), 1484 (m), 1435 (w), 1412 (m), 1378 (w), 1325 (s), 1298 (w), 1269 (m), 1236 (w), 1168 (m), 1135 (s), 1076 (m), 1039 (w), 1014 (w), 985 (w), 958 (w), 927 (m), 851 (m), 790 (w), 766 (w), 728 (s), 673 (m), 628

https://doi.org/10.1021/acs.organomet.2c00492
Organometallics 2022, 41, 3852−3860

(w), 590 (w), 577 (w), 553 (w), 535 (w), 504 (w), 478 (m), 446 (w) cm^{-1}. HRMS ESI; *m/z* calcd for $C_{18}H_{16}F_3N_3Se_1$ $[M + Na]^+$: 434.0354, found: 434.0352.

*1-Mesityl-3-(5-(trifluoromethyl)pyridin-2-yl)-1,3-dihydro-2H-benzo[d]imidazole-2-selenone (**2b**).* Following the general procedure, selenium-benzimidazole **2b** (19.7 mg, 0.04 mmol, 40%) was obtained as an off-white solid from the corresponding compound **1b** (50.0 mg, 0.11 mmol). ^{1}H NMR (300 MHz, $CDCl_3$): δ = 8.97 (s, 1H), 8.68 (d, J = 8.5 Hz, 1H), 8.20 (d, J = 8.4 Hz, 1H), 7.65 (d, J = 7.6 Hz, 1H), 7.33−7.23 (s, 2H), 7.10 (s, 2H), 6.84 (d, J = 7.6 Hz, 1H), 2.40 (s, 3H), 2.04 (s, 6H) ppm. ^{13}C NMR (75 MHz, $CDCl_3$): δ = 167.00, 153.30, 146.14 ($J_{C,F}$ = 4.1 Hz), 140.06, 136.28, 135.30 ($J_{C,F}$ = 3.3 Hz), 133.72, 132.92, 131.18, 129.86 (2C), 126.40 ($J_{C,F}$ = 33.6 Hz), 125.06, 124.47, 123.45, 123.30 ($J_{C,F}$ = 272.5 Hz), 112.52, 110.27, 21.43, 18.20 (2C) ppm. ^{19}F NMR (282 MHz, $CDCl_3$): δ = −62.23 (s, CF_3) ppm. ^{77}Se NMR (57 MHz, $CDCl_3$): δ = 140.62 (s, C=*Se*) ppm. IR (neat): $\tilde{\nu}$ = 2919 (w), 2852 (w), 1726 (w), 1598 (m), 1580 (w), 1486 (w), 1471 (m), 1401 (w), 1376 (m), 1319 (s), 1302 (w), 1276 (m), 1209 (w), 1166 (w), 1126 (s), 1076 (m), 1036 (w), 1015 (m), 931 (w), 849 (w), 831 (m), 772 (w), 741 (s), 682 (w), 665 (w), 645 (w), 619 (m), 564 (w), 544 (w), 508 (w), 448 (w), 420 (w) cm^{-1}. HRMS ESI; *m/z* calcd for $C_{22}H_{18}F_3N_3Se_1$ $[M + Na]^+$: 484.0511, found: 484.0510.

*5,6-Dichloro-1-mesityl-3-(5-(trifluoromethyl)pyridin-2-yl)-1,3-dihydro-2H-benzo[d]imidazole-2-selenone (**2c**).* Following the general procedure, selenium-imidazole **2c** (53.3 mg, 0.10 mmol, 99%) was obtained as an off-white solid from the corresponding compound **1c** (60.0 mg, 0.10 mmol). ^{1}H NMR (300 MHz, $CDCl_3$): δ = 8.98 (s, 1H), 8.74 (d, J = 8.5 Hz, 1H), 8.20 (d, J = 8.4 Hz, 1H), 7.84 (s, 1H), 7.11 (s, 2H), 6.90 (s, 1H), 2.41 (s, 3H), 2.03 (s, 6H) ppm. ^{13}C NMR (75 MHz, $CDCl_3$): δ = 168.84, 152.70, 146.17 ($J_{C,F}$ = 4.1 Hz), 140.57, 136.12, 135.44 ($J_{C,F}$ = 3.3 Hz), 133.02, 131.81, 130.42, 130.05 (2C); 129.51, 128.77, 126.65 ($J_{C,F}$ = 33.6 Hz), 123.16 ($J_{C,F}$ = 272.7 Hz), 122.88, 114.28, 111.01, 21.42, 18.16 (2C) ppm. ^{19}F NMR (282 MHz, $CDCl_3$): δ = −62.27 (s, CF_3) ppm. ^{77}Se NMR (57 MHz, $CDCl_3$): δ = 188.43 (s, C=*Se*) ppm. IR (neat): $\tilde{\nu}$ = 3067 (w), 2920 (w), 2853 (w), 1736 (w), 1598 (m), 1574 (w), 1484 (w), 1464 (m), 1434 (w), 1398 (w), 1372 (m), 1353 (w), 1323 (m), 1305 (w), 1273 (m), 1228 (w), 1208 (w), 1164 (m), 1129 (s), 1100 (w), 1075 (m), 1013 (w), 986 (w), 931 (w), 887 (w), 857 (m), 773 (w), 739 (w), 701 (w), 682 (w), 656 (w), 598 (w), 561 (m), 522 (w), 500 (w), 483 (w), 454 (w), 426 (w) cm^{-1}. HRMS ESI; *m/z* calcd for $C_{22}H_{16}Cl_2F_3N_3Se_1$ $[M + Na]^+$: 551.9727, found: 551.9727.

General Procedure for the Hetero-Diels−Alder Reaction. After a slightly modified procedure from Meggers et al.,[13] a Schlenk tube was charged with β,γ-unsaturated α-ketoester (0.2 mmol) and **Λ-Fe1-3** (0.006 mmol, 3 mol%), and then the flask was purged with nitrogen. Then, distilled CH_2Cl_2 (4.0 mL, 0.05 M) was added followed by dihydrofuran (0.3 mmol). The flask was sealed and stirred at room temperature for 24 h. Afterward, the reaction mixture was filtered over a short plug of silica with CH_2Cl_2 to remove the remaining catalyst, so the dr of the crude product could be determined. The crude product was purified via silica gel column chromatography (*n*-pentane/EtOAc 5:1) to afford the desired product bicyclic product (3a*S*,4*S*,7a*R*)-**5** as a colorless oil. The dr was determined by ^{1}H NMR spectroscopy of the crude product and by HPLC analysis on a chiral stationary phase of the isolated product. Enantiomeric excess was established by HPLC analysis on a chiral stationary phase. HPLC conditions: Daicel Chiralpak IB column, 250 mm × 4.6 mm, absorbance at 254 nm, mobile phase *n*-hexane/isopropanol = 90:10, isocratic flow, flow rate 1.0 mL/min, 25 °C, t_r (major) = 10.96 min, t_r (minor) = 9.78 min. TLC (*n*-pentane/EtOAc 5:1): R_f = 0.27. ^{1}H NMR (300 MHz, $CDCl_3$): δ = 7.37−7.29 (m, 3H), 7.26−7.21 (m, 2H), 6.23−6.19 (m, 1H), 5.65 (d, J = 3.4 Hz, 1H), 4.21−4.16 (m, 2H), 3.91−3.82 (m, 4H), 2.71−2.64 (m, 1H), 1.72 (q, J = 10.8 Hz, 1H), 1.40−1.31 (m, 1H) ppm. ^{13}C NMR (75 MHz, $CDCl_3$): δ = 163.07, 142.63, 141.12, 128.79 (2C), 127.68 (2C), 127.17, 110.19, 101.46, 68.60, 52.48, 44.08, 38.25, 24.70 ppm. The spectroscopic and HPLC data of the dihydropyran **5** are in agreement with the literature.[13,17]

■ ASSOCIATED CONTENT

Supporting Information

The Supporting Information is available free of charge at https://pubs.acs.org/doi/10.1021/acs.organomet.2c00492.

Synthesis of ligands, NMR spectra, HPLC traces, and crystallographic data (PDF)

Accession Codes

CCDC 2209632 contains the supplementary crystallographic data for this paper. These data can be obtained free of charge via www.ccdc.cam.ac.uk/data_request/cif, or by emailing data_request@ccdc.cam.ac.uk, or by contacting The Cambridge Crystallographic Data Centre, 12 Union Road, Cambridge CB2 1EZ, UK; fax: +44 1223 336033.

■ AUTHOR INFORMATION

Corresponding Author

Eric Meggers − *Fachbereich Chemie, Philipps-Universität Marburg, 35043 Marburg, Germany;* orcid.org/0000-0002-8851-7623; Email: meggers@chemie.uni-marburg.de

Authors

Nemrud Demirel − *Fachbereich Chemie, Philipps-Universität Marburg, 35043 Marburg, Germany*

Jakob Haber − *Fachbereich Chemie, Philipps-Universität Marburg, 35043 Marburg, Germany*

Sergei I. Ivlev − *Fachbereich Chemie, Philipps-Universität Marburg, 35043 Marburg, Germany;* orcid.org/0000-0003-4871-825X

Complete contact information is available at: https://pubs.acs.org/10.1021/acs.organomet.2c00492

Notes

The authors declare no competing financial interest.

■ ACKNOWLEDGMENTS

This project received funding from the European Research Council (ERC) under the European Union's Horizon 2020 research and innovation programme (grant agreement no. 883212).

■ REFERENCES

(1) Anastas, P.; Eghbali, N. Green Chemistry: Principles and Practice. *Chem. Soc. Rev.* **2010**, *39*, 301−312.

(2) For recent special issues on the catalysis with earth-abundant metals, see: (a) Chirik, P.; Morris, R. Getting Down to Earth: The Renaissance of Catalysis with Abundant Metals. *Acc. Chem. Res.* **2015**, *48*, 2495. (b) Beller, M. Introduction: First Row Metals and Catalysis. *Chem. Rev.* **2019**, *119*, 2089.

(3) For selected reviews on iron catalysis, see: (a) Bolm, C.; Legros, J.; Le Paih, J.; Zani, L. Iron-Catalyzed Reactions in Organic Synthesis. *Chem. Rev.* **2004**, *104*, 6217−6254. (b) Enthaler, S.; Junge, K.; Beller, M. Sustainable Metal Catalysis with Iron: From Rust to a Rising Star? *Angew. Chem., Int. Ed.* **2008**, *47*, 3317−3321. (c) Bauer, I.; Knölker, H.-J. Iron Catalysis in Organic Synthesis. *Chem. Rev.* **2015**, *115*, 3170−3387. (d) Fürstner, A. Iron Catalysis in Organic Synthesis: A Critical Assessment of What It Takes To Make This Base Metal a Multitasking Champion. *ACS Cent. Sci.* **2016**, *2*, 778−789. (e) Shang, R.; Ilies, L.; Nakamura, E. Iron-Catalyzed C−H Bond Activation. *Chem. Rev.* **2017**, *117*, 9086−9139. (f) Piontek, A.; Bisz, E.; Szostak, M. Iron-Catalyzed Cross-Couplings in the Synthesis of Pharmaceuticals: In Pursuit of Sustainability. *Angew. Chem., Int. Ed.* **2018**, *57*, 11116−11128. (g) DaBell, P.; Thomas, S. P. Iron Catalysis in Target

Synthesis. *Synthesis* **2020**, *52*, 949−963. (h) Liu, Y.; You, T.; Wang, H.-X.; Tang, Z.; Zhou, C.-Y.; Che, C.-M. Iron- and cobalt-catalyzed C(sp^3)−H bond functionalization reactions and their application in organic synthesis. *Chem. Soc. Rev.* **2020**, *49*, 5310−5358. (i) Fusi, G. M.; Gazzola, S.; Piarulli, U. Chiral Iron Complexes in Asymmetric Organic Transformations. *Adv. Synth. Catal.* **2022**, *364*, 696−714.

(4) For selected reviews on asymmetric iron catalysis, see: (a) Gopalaiah, K. Chiral Iron Catalysts for Asymmetric Synthesis. *Chem. Rev.* **2013**, *113*, 3248−3296. (b) Ollevier, T.; Keipour, H. Enantioselective Iron Catalysts. In *Iron Catalysis II*; Bauer, E., Ed.; Springer International Publishing: Cham, 2015; pp 259−309. (c) Pellissier, H. Recent developments in enantioselective iron-catalyzed transformations. *Coord. Chem. Rev.* **2019**, *386*, 1−31. (d) Casnati, A.; Lanzi, M.; Cera, G. Recent Advances in Asymmetric Iron Catalysis. *Molecules* **2020**, *25*, 3889.

(5) For reviews on different aspects of metal-centered chirality, see: (a) Pierre, J.-L. Enantioselective creation of helical chirality in octahedral (OC-6) complexes. Recent advances. *Coord. Chem. Rev.* **1998**, *178-180*, 1183−1192. (b) Brunner, H. Optically Active Organometallic Compounds of Transition Elements with Chiral Metal Atoms. *Angew. Chem., Int. Ed.* **1999**, *38*, 1194−1208. (c) Knof, U.; von Zelewsky, A. Predetermined Chirality at Metal Centers. *Angew. Chem., Int. Ed.* **1999**, *38*, 302−322. (d) Knight, P. D.; Scott, P. Predetermination of chirality at octahedral centres with tetradentate ligands: prospects for enantioselective catalysis. *Coord. Chem. Rev.* **2003**, *242*, 125−143. (e) Ganter, C. Chiral organometallic half-sandwich complexes with defined metal configuration. *Chem. Soc. Rev.* **2003**, *32*, 130−138. (f) Fontecave, M.; Hamelin, O.; Ménage, S. Chiral-at-Metal Complexes as Asymmetric Catalysts. *Top. Organomet. Chem.* **2005**, *15*, 271−288. (g) Meggers, E. Asymmetric Synthesis of Octahedral Coordination Complexes. *Eur. J. Inorg. Chem.* **2011**, *2011*, 2911−2926. (h) Bauer, E. B. Chiral-at-metal complexes and their catalytic applications in organic synthesis. *Chem. Soc. Rev.* **2012**, *41*, 3153−3167. (i) Constable, E. C. Stereogenic metal centres − from Werner to supramolecular chemistry. *Chem. Soc. Rev.* **2013**, *42*, 1637−1651. (j) von Zelewsky, A. Stereochemistry of Coordination Compounds. From Alfred Werner to the 21st Century. *Chimia* **2014**, *68*, 297−298. (k) Gong, L.; Chen, L.-A.; Meggers, E. Asymmetric Catalysis Mediated by the Ligand Sphere of Octahedral Chiral-at-Metal Complexes. *Angew. Chem., Int. Ed.* **2014**, *53*, 10868−10874. (l) Cruchter, T.; Larionov, V. A. Asymmetric catalysis with octahedral stereogenic-at-metal complexes featuring chiral ligands. *Coord. Chem. Rev.* **2018**, *376*, 95−113.

(6) Zhang, L.; Meggers, E. Stereogenic-Only-at-Metal Asymmetric Catalysts. *Chem. Asian J.* **2017**, *12*, 2335−2342.

(7) Zhang, L.; Meggers, E. Steering Asymmetric Lewis Acid Catalysis Exclusively with Octahedral Metal-Centered Chirality. *Acc. Chem. Res.* **2017**, *50*, 320−330.

(8) Huang, X.; Meggers, E. Asymmetric Photocatalysis with Bis-cyclometalated Rhodium Complexes. *Acc. Chem. Res.* **2019**, *52*, 833−847.

(9) Huo, H.; Fu, C.; Harms, K.; Meggers, E. Asymmetric Catalysis with Substitutionally Labile yet Stereochemically Stable Chiral-at-Metal Iridium(III) Complex. *J. Am. Chem. Soc.* **2014**, *136*, 2990−2993.

(10) Wang, C.; Chen, L.-A.; Huo, H.; Shen, X.; Harms, K.; Gong, L.; Meggers, E. Asymmetric Lewis acid catalysis directed by octahedral rhodium centrochirality. *Chem. Sci.* **2015**, *6*, 1094−1100.

(11) Zheng, Y.; Tan, Y.; Harms, K.; Marsch, M.; Riedel, R.; Zhang, L.; Meggers, E. Octahedral Ruthenium Complex with Exclusive Metal-Centered Chirality for Highly Effective Asymmetric Catalysis. *J. Am. Chem. Soc.* **2017**, *139*, 4322−4325.

(12) Hong, Y.; Jarrige, L.; Harms, K.; Meggers, E. Chiral-at-Iron Catalyst: Expanding the Chemical Space for Asymmetric Earth-Abundant Metal Catalysis. *J. Am. Chem. Soc.* **2019**, *141*, 4569−4572.

(13) Hong, Y.; Cui, T.; Ivlev, S.; Xie, X.; Meggers, E. Chiral-at-Iron Catalyst for Highly Enantioselective and Diastereoselective Hetero-Diels-Alder Reaction. *Chem. - Eur. J.* **2021**, *27*, 8557−8563.

(14) (a) Meggers, E. Chiral Auxiliaries as Emerging Tools for the Asymmetric Synthesis of Octahedral Metal Complexes. *Chem. - Eur. J.* **2010**, *16*, 752−758. (b) Gong, L.; Wenzel, M.; Meggers, E. Chiral-Auxiliary-Mediated Asymmetric Synthesis of Ruthenium Polypyridyl Complexes. *Acc. Chem. Res.* **2013**, *46*, 2635−2644. (c) Ma, J.; Zhang, X.; Huang, X.; Luo, S.; Meggers, E. Preparation of chiral-at-metal catalysts and their use in asymmetric photoredox chemistry. *Nat. Protoc.* **2018**, *13*, 605−632.

(15) (a) Liske, A.; Verlinden, K.; Buhl, H.; Schaper, K.; Ganter, C. Determining the π-Acceptor Properties of N-Heterocyclic Carbenes by Measuring the ^{77}Se NMR Chemical Shifts of Their Selenium Adducts. *Organometallics* **2013**, *32*, 5269−5272. (b) Verlinden, K.; Buhl, H.; Frank, W.; Ganter, C. Determining the Ligand Properties of N-Heterocyclic Carbenes from ^{77}Se NMR Parameters. *Eur. J. Inorg. Chem.* **2015**, *2015*, 2416−2425. (c) Vummaleti, S. V. C.; Nelson, D. J.; Poater, A.; Gomez-Suarez, A.; Cordes, D. B.; Slawin, A. M. Z.; Nolan, S. P.; Cavallo, L. What can NMR spectroscopy of selenoureas and phosphinidenes teach us about the π-accepting abilities of N-heterocyclic carbenes? *Chem. Sci.* **2015**, *6*, 1895−1904.

(16) (a) Yadav, S.; Deka, R.; Singh, H. B. Recent Developments in the Chemistry of NHC-based Selones: Syntheses, Applications and Reactivity. *Chem. Lett.* **2019**, *48*, 65−79. (b) Jamil, M. S. S.; Alkaabi, S.; Brisdon, A. K. Simple NMR predictors of catalytic hydrogenation activity for [Rh(cod)Cl(NHC)] complexes featuring fluorinated NHC ligands. *Dalton Trans.* **2019**, *48*, 9317−9327. (c) Makhloufi, A.; Wahl, M.; Frank, W.; Ganter, C. A New Mixed Amino-Amido N-Heterocyclic Carbene Based on Anthranilic Acid. *Organometallics* **2013**, *32*, 854−861.

(17) Zhu, Y.; Xie, M.; Dong, S.; Zhao, X.; Lin, L.; Liu, X.; Feng, X. Asymmetric Cycloaddition of β,γ-Unsaturated α-Ketoesters with Electron-Rich Alkenes Catalyzed by a Chiral $Er(OTf)_3$/*N*,*N*′-Dioxide Complex: Highly Enantioselective Synthesis of 3,4-Dihydro-2*H*-pyrans. *Chem. - Eur. J.* **2011**, *17*, 8202−8208.

https://doi.org/10.1021/acs.organomet.2c00492
Organometallics 2022, 41, 3852−3860